Productive Synthesis and Properties of Polydiaminoanthraquinone and Its Pure Self-Stabilized Nanoparticles with Widely Adjustable Electroconductivity

Xin-Gui Li,* Hu Li, and Mei-Rong Huang[a]

Abstract: Wholly aromatic poly(1,5-diaminoanthraquinone) (PDAA) particles were productively synthesized for the first time by chemically oxidative polymerization of 1,5-diaminoanthraquinone (DAA) by using CrO_3, $K_2Cr_2O_7$, K_2CrO_4, or $KMnO_4$ as oxidants in acidic DMF. The effects of the oxidant species, oxidant/DAA ratio, polymerization temperature, and medium on the polymerization yield, macromolecular structure, size, electroconductivity, solubility, solvatochromism, thermostability, photoluminescence, and silver-ion sorption of the PDAA particles were systematically studied by IR, UV/Vis, fluorescence, and solid-state ^{13}C NMR spectroscopies, wide-angle X-ray diffraction, scanning and transmission electron microscopies, and laser particle-size, differential scanning calorimetry (DSC), and thermal gravimetric (TG) analyses. It seems that the DAA is oxidatively polymerized at the 1,4- and 5,8-positions. Surprisingly, the chemical oxidative polymerization of DAA with CrO_3 at 0 °C in H_2SO_4/DMF in the absence of external stabilizer simply affords novel PDAA nanoparticles of around 30 nm in diameter with high purity, clean surfaces, inherent semiconductivity, and self-stability that can be ascribed to the presence of a large number of 1,4-benzoquinone units that are negatively charged on their macromolecular chains. The polymers exhibit a high thermal stability at temperatures below 400 °C. Two unique nanoeffects were found, namely the strongest silver-ion adsorbability and photoluminescence of the PDAA nanoparticles. This gives a facile and general route for the application of the versatilities of PDAA nanomaterials. The PDAA particles are good semiconductors with a widely adjustable conductivity that moves across seven orders of magnitude through simple $HClO_4$ redoping or Ag^+ sorption, as expected.

Keywords: conducting materials · nanoparticles · nanotechnology · polymerization · structure–property relationships

Introduction

Novel conducting π-conjugated polymers such as polyaniline, polypyrrole, and their derivatives have been extensively studied for chemical, electronic, optical, magnetic, and biological applications, because their electroconductivity, electrochromism, electrocatalysis, electroactivity, optical activity, and ion adsorbability can be facilely controlled by a reversible acid-doping/alkali-dedoping treatment.[1,2] Moreover,

[a] Prof. Dr. X.-G. Li, H. Li, Prof. M.-R. Huang
Institute of Materials Chemistry
Key Laboratory of Advanced Civil Engineering Materials
College of Materials Science and Engineering
Tongji University
1239 Siping Road, Shanghai 200092 (China)
Fax: (+86)21-65980524
E-mail: adamxgli@yahoo.com

Supporting information for this article is available on the WWW under http://www.chemeurj.org/ or from the author.

conducting polymer nanomaterials (for example, nanoparticles, nanowires, nanofilms, and nanocomposites) have attracted much attention, with the expectation that such polymers will possess the advantages of both organic semiconductors and nanomaterials.[3–5] In recent years, a new kind of wholly aromatic polymer called poly(1,5-diaminoanthraquinone) (PDAA) has been synthesized by electropolymerization.[6,7] PDAA contains a moiety of 1,4-benzoquinone condensed between two moieties of aniline, and it has higher electroactivity than polyaniline because of the hybridization part.[6] A hybridization moiety, for example, quinone (Q/$Q^{\bullet-}$/Q^{2-}) in a π-conjugated system, may give even higher electroactivity than just the simple mixture or the conducting polymer alone. Therefore, the polymer with 1,4-benzoquinone groups is anticipated as a multifunctional material that presents better properties than conventional conducting polymers and could serve as a new advanced material with wide potential applicability.[8]

The aromatic amine polymer with 1,4-benzoquinone units, as a typical multifunctional hybridizable material, exhibits some novel properties similar to other hybrid materials. It is reported that 1,5-diaminoanthraquinone (DAA) and its derivatives can electropolymerize into thin compact polymer films with an even surface, as well as good specific capacity.[7] However, the area, shape, and productivity of the films depend completely on the characteristics of the electrode used. In fact, a large-area film could not be easily and productively obtained by electropolymerization. Additionally, the poor solubility of the DAA polymers greatly limits their practical applications. Fortunately, it has been found that the preparation of submicrometer- or nanoscale materials is one of the attractive alternatives to overcome the poor processability. Besides, submicron- or nanomaterials have become another important subject in conducting polymers because of their important electrical properties, unique nanoeffects, and numerous potential applications, such as in conducting nanocomposites with low percolation thresholds,[9] metal anticorrosion coatings,[10] electrode modifiers,[11] luminescent materials, and advanced sorbents. In particular, conducting polymer particles as effective sorbents can efficiently adsorb and recover the noble silver ions and harmful lead ions from waste water.[12] On the other hand, the adsorption of silver ions onto the particles facilely and directly affords the formation of a silver nanocomposite with enhanced functionalities. Therefore, a chemically oxidative polymerization should be carefully designed and optimized for the fabrication of submicrometer- or nanosized particles of DAA polymers, in order to successfully resolve the problems of poor processability, low productivity, and electrode limitations. Unfortunately, no study has focused on this at all until now.

In this study, the chemical oxidative polymerization of the DAA monomer has been carried out. The polymerization is a new method to productively produce the wholly aromatic PDAA microparticles and nanoparticles with high purity, clean surfaces, inherent self-stability, and adjustable conductivity. The polymerization characteristics, molecular and morphological structures, and multifunctionalities of the DAA polymer were systematically elaborated. A new technique to facilely prepare pure polymer nanoparticles with a diameter of around 30 nm by a simple polymerization in acidic organic medium without external additives or internal ionic side groups as a stabilizer is proposed.

Results and Discussion

Synthesis of the poly(1,5-diaminoanthraquinone) particles: The chemical oxidative polymerization of the DAA monomer simply afforded a dark precipitate as the product. The color of the product changed from brown to black with oxidant species. The polymerization process was followed by in situ measurement of the open circuit potential (OCP) and the temperature of the reaction solution, which may provide a deeper insight into the polymerization process (see Figure S2 in the Supporting Information). The initial OCP of the DAA monomer in acidic DMF solution was 480 mV versus the saturated calomel electrode (SCE). This value was the equilibrium potential for the protonated DAA monomer after a time lapse of 30 min. The initial polymerization OCP is somewhat higher than those of aniline and its derivatives, possibly due to the intrinsically high oxidation potential of DAA itself. The solution potential dramatically increased from 482 to 854 mV versus SCE with addition of oxidant solution during the first 12 min of the reaction. After a relatively stable potential of 854 mV for another 10 min, a gradual potential decline to 652 mV versus SCE at about 130 min and to 505 mV versus SCE at 600 min at a very low rate was observed. The variation of the potential suggests three stages of polymerization, that is, increasing, relatively steady, and decreasing. During the first stage, the polymerization may be fast because of the quickly rising rate of the potential. During the second stage, the polymer chains formed at this stage may be further oxidized by the remnant oxidant and also newly added oxidant. The chain propagation may continue on the oxidized chains to form a higher-molecular-weight polymer. These as-formed polymer chains may also be oxidized to participate in the chain propagation. This process is repeated many times until all of the oxidant is consumed at the end of the plateau stage. In the third stage, the OCP decays slowly from the maximum potential, but it is hard for it to decline to the initial potential. This stage should include further polymerization of monomers, with the oxidized polymer chain that previously formed as the oxidant. The polymerization stages of the DAA monomer in the OCP plot are very similar to the situation observed for the chemical oxidative polymerization of aniline and its derivatives.[13–15] However, only a slight change of the polymerization solution temperature was detected, except for a small rise in the temperature at the initial polymerization time of about 22 min, which is quite different from the polymerization of aniline and its derivatives with an obviously exothermic tendency. This may be due to a great difference between the reactant concentrations. The monomer and oxidant concentrations in this study are much lower than those in reference [15].

The influence of the oxidant species and its standard reduction potential (RP) on the polymerization yield, conductivity, and solubility of the DAA polymers obtained has been systematically studied. It was found that the yield, conductivity, and solubility all vary significantly as the oxidant is changed between $(NH_4)_2S_2O_8$ (RP = 2.01), $Na_2S_2O_8$ (2.01), H_2O_2 (1.77), $KMnO_4$ (1.51), CrO_3 (1.35), $K_2Cr_2O_7$ (1.33), K_2CrO_4 (1.20), $NaClO_4$ (1.19), and $FeCl_3$ (0.77) with different RP values. No polymer was obtained or the polymerization solution did not turn dark if $(NH_4)_2S_2O_8$, $Na_2S_2O_8$, H_2O_2, and $NaClO_4$ were used as oxidants for the DAA polymerization. When $FeCl_3$ (with the lowest RP value) was used, the resultant polymerization solution did turn dark, but no solid polymer was attained by filtration, a result suggesting the formation of some soluble oligomers in acidic DMF. Another four oxidants, namely $KMnO_4$, CrO_3,

Table 1. The effect of oxidant species on the polymerization yield, bulk electrical conductivity, and solubility of poly(1,5-diaminoanthraquinone) (PDAA) salts formed with an oxidant/DAA molar ratio of 1:1 in 1 M H_2SO_4/DMF solution at 20 °C for 24 h.

Oxidants		$KMnO_4$	CrO_3	$K_2Cr_2O_7$	K_2CrO_4
polymerization yield [%]		21.4	52.4	31.3	43.5
electrical conductivity [S cm^{-1}]	virgin H_2SO_4-doped salt	1.06×10^{-6}	5.54×10^{-6}	2.71×10^{-9}	3.04×10^{-9}
	NH_4OH-dedoped base	3.24×10^{-7}	1.21×10^{-7}	7.85×10^{-11}	9.38×10^{-11}
	$HClO_4$-redoped salt[c]	2.21×10^{-5}	6.45×10^{-5}	3.34×10^{-7}	5.35×10^{-6}
solubility[a] and solution color[b] of the PDAA salts	H_2SO_4 (101)[d]	S, bl	S, bl	S, bl	S, bl
	H_2O (80)[d]	IS	IS	IS	IS
	HCOOH (58)[d]	S, g	PS, g	PS, p	SS
	DMSO (47)[d]	MS, bp	PS, b	SS	PS, p
	NMP (32)[d]	MS, b	PS, b	PS, b	SS
	m-Cresol (12)[d]	MS, bp	PS, bp	IS	IS
	THF (7)[d]	PS, bp	SS	IS	SS
	CHCl$_3$ (5)[d]	PS, y	SS	IS	IS
	HCl or NaOH in H_2O	IS	IS	IS	IS

[a] IS: insoluble; MS: mainly soluble; PS: partially soluble; S: soluble; SS: slightly soluble. DAA monomer is completely soluble in H_2SO_4, HCOOH, DMSO, N-methylpyrrolidone (NMP), m-cresol, DMF, THF, and CHCl$_3$ and displays a red solution, but it is insoluble in H_2O, HCl, and NaOH. [b] b: blue; bl: black; bp: bluish purple; g: green; p: purple; y: yellow. [c] The dedoped particles of the PDAAs were redoped in 1 M HClO$_4$ aqueous solution for 24 h. [d] The value in brackets is dielectric constant of the solvents.

to 3.0, the yield increases slowly from 66.4 up to 75.6%. The polymer has a maximum conductivity at an oxidant/monomer molar ratio of 1.0. At lower oxidant contents, the oxidant was consumed very quickly, so that not enough oxidant was used to oxidize the residual monomers for further polymerization and chain propagation. This resulted in much lower yield and conductivity. When more oxidant was added, more monomer could be oxidized and then more chain initiation and propagation would occur, finally leading to the formation of more polymers with higher conductivity. However, too much oxidant would produce more
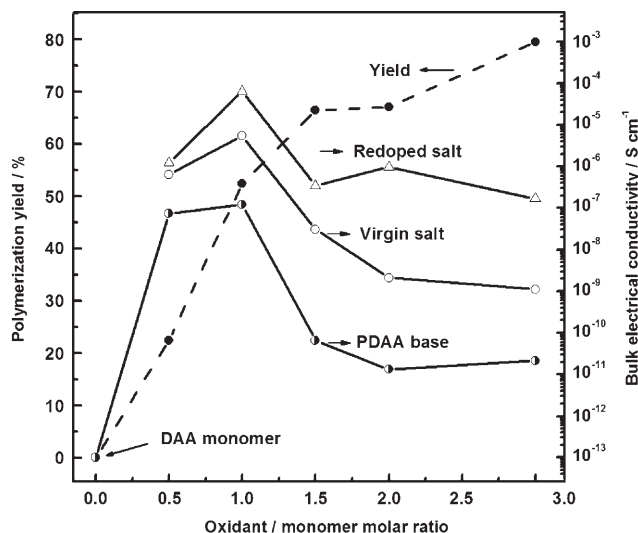
$K_2Cr_2O_7$, and K_2CrO_4, with moderate RP values ranging from 1.20–1.51 mV can produce dark precipitates as polymerization products, as listed in Table 1. Although there is no regular relationship between the RP values, yields, and properties, it is certain that CrO_3 is the optimal oxidant to prepare PDAA, with the highest polymerization yield (52.4%), the highest conductivity (6.45×10^{-5} S cm^{-1}), and the second best solubility. This indicates an effective oxidizability of CrO_3 on the DAA monomers for oxidative polymerization in acidic organic solution. The lowest yield, the second highest conductivity, but the strongest solubility were observed when $KMnO_4$ (with the highest RP value) of the four efficient oxidants was employed as an oxidant. That is to say, the polymer obtained with $KMnO_4$ might undergo a degradation reaction, thereby leading to the formation of some oligomers that are soluble in the polymerization medium and finally to the lowest yield and the highest solubility. The polymers obtained with K_2CrO_4 and $K_2Cr_2O_7$ show poor solubility and low conductivity.[16] Therefore, it should be noted that the RP values and the chemical structures of the oxidants play an important role in the oxidative polymerization of the DAA monomer. RP values that are either too high or too low are not appropriate for the polymerization. This implies that the oxidation (radical cation) and further polymerization processes of the DAA monomer containing oxidizable NH_2 and reducible C=O groups must have a complicated mechanism. This mechanism is quite different from the polymerization mechanism of aniline containing only oxidizable NH_2 groups.[16]

The effect of the oxidant/monomer ratio on DAA polymerization is shown in Figure 1. With an increase in the oxidant/monomer molar ratio from 0 up to 1.5, the polymerization yield increases rapidly from 0 up to 66.4%. As the oxidant/monomer molar ratio further increases from 1.5 up

Figure 1. Variation of the polymerization yield and bulk electrical conductivity of the PDAA polymers with the oxidant (CrO_3)/DAA monomer molar ratio in 1 M H_2SO_4 in DMF at 20 °C for 24 h. Redoped salt was obtained with 1 M HClO$_4$ aqueous solution as the redopant.

oligomers with lower conductivity.[17] Apparently, the optimal oxidant/monomer molar ratio should be 1.0 for the synthesis of PDAA with moderate yield (52.4%) and the highest conductivity.

As shown in Figure 2, with elevating polymerization temperatures from 0 up to 50 °C, the yield and conductivity of the polymer exhibit maximum values at 10 and 20 °C, respectively. Obviously, a relatively low temperature is favorable for the growth of the polymer chain, because too high a temperature would induce more chain termination but too low a temperature might cause a slower reaction and less chain initiation. Certainly, 10–20 °C is the optimal tempera-
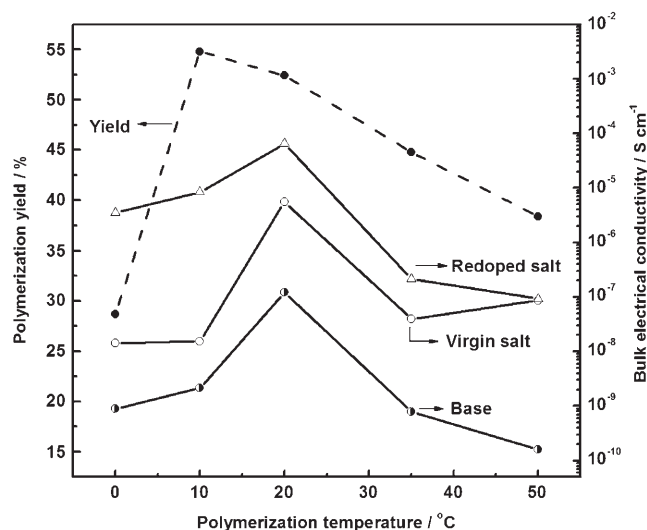
Figure 2. Influence of the polymerization temperature on the polymerization yield and bulk electrical conductivity of the virgin salt, base, and 1 M HClO$_4$-redoped salt of the PDAA particles obtained with a CrO$_3$/DAA molar ratio of 1:1 in 1 M H$_2$SO$_4$ in DMF for 24 h.

ture for the preparation of PDAA with high yield and conductivity, possibly due to the proper initiation and propagation rates. A very similar relationship between polymer temperature, yield, and conductivity has been found for the chemical oxidative polymerization of aniline and 4-sulfonic diphenylamine.[18]

The significant influence of the acid species at 1.0 M in DMF on the DAA polymerization was also investigated. The yield was found to rise from 8.9 to 46.8, 47.5, 48.5, or 52.4% upon changing the acid from H$_3$PO$_4$ to HCl, HNO$_3$, HClO$_4$, or H$_2$SO$_4$, respectively (see Table S1 in the Supporting Information). The polymer obtained in H$_3$PO$_4$/DMF exhibits the lowest yield, probably because this mixture has the lowest H$^+$ concentration in all five acid media. Although the yields are similar for the other four acids, HClO$_4$ seems the optimal acid, which creates the polymer with the highest conductivity in all kinds of acid solutions, as discussed below.

Besides the nature of the acid, the concentration of the acid in DMF also remarkably affects the polymerization characteristics. Figure 3 shows that the polymerization yield exhibits a maximum at an H$_2$SO$_4$ concentration of 1.0 M. The polymerization cannot proceed in acid-free DMF because of the very weak oxidative ability of the oxidant (CrO$_3$) in neutral or basic solvent or because of the absence of the vital protonation of the NH$_2$ groups before the oxidative polymerization. On the other hand, the polymerization at a higher H$_2$SO$_4$ concentration of 2.0 M produces a lower yield, which indicates that the higher acid concentration results in more chain degradation due to acidolysis. As canvassed below, a very similar relationship between the H$_2$SO$_4$ concentration and conductivity has been observed. The dependence of the yield and conductivity of the PDAA on the H$_2$SO$_4$ concentration clearly illustrates that two competing
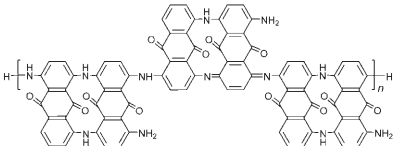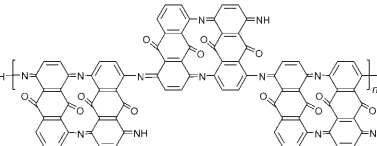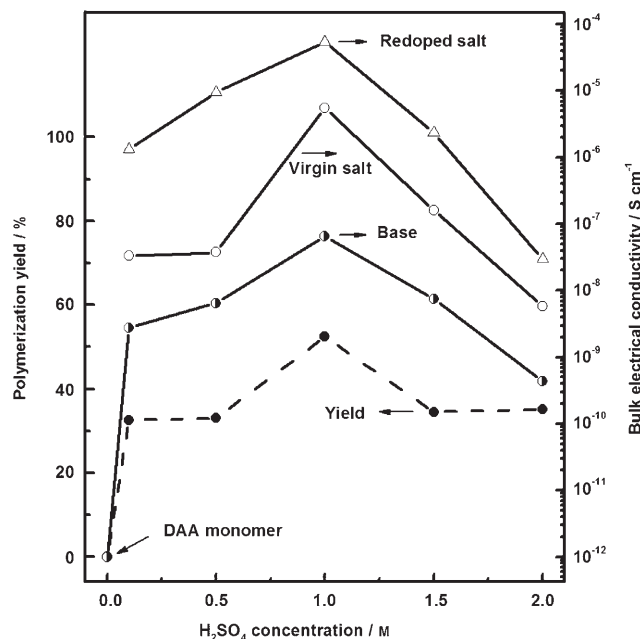

Figure 3. Effect of H$_2$SO$_4$ concentration on the polymerization yield and bulk electrical conductivity of the virgin salt, base, and 1 M HClO$_4$-redoped salt of the PDAA particles obtained with a CrO$_3$/DAA monomer molar ratio of 1:1 in H$_2$SO$_4$ in DMF at 20°C for 24 h.

processes (chain propagation and acidolysis) control the polymerization. In summary, the species and concentration of the acid greatly influence the polymerization and the properties of the resultant PDAA.

Structure of the PDAA polymers: It appears that no reports concerning the structure analysis of PDAA polymers obtained by chemical oxidative polymerization have been made until now because the PDAA polymer particles are not totally soluble in most solvents. Therefore, the structure characterization must be performed by solid-state techniques including elemental analysis, FTIR spectroscopy, solid-state high-resolution ^{13}C NMR spectroscopy, and wide-angle X-ray diffraction (WAXD). Fortunately, UV/Vis spectroscopy can be used as an additional analytical method since the fine particles of PDAA bases can steadily be dispersed in NMP by ultrasonic treatment.

The macromolecular structure of the PDAA polymers has been studied by elemental analysis because a certain C/H/N/O ratio must reveal a molecular structure. The two groups of C/H/N/O ratios listed in Table 2 suggest two proposed formulas of the PDAA polymers oxidized by CrO$_3$ and K$_2$CrO$_4$. Obviously, the experimental C/H/N/O ratio determined by elemental analysis is very close to the ratio of the proposed formulas. It is seen that there are more NH/NH$_2$ groups and C=C benzenoid rings in PDAA oxidized by CrO$_3$, whereas there are much fewer NH/NH$_2$ groups but more C=C quinoid rings in PDAA oxidized by K$_2$CrO$_4$. This difference of the chain structures has been further confirmed by much lower solubility (Table 1) and a stronger C=C quinoid band in the IR spectrum (Figure 4) of the latter.

Table 2. Elemental analysis and proposed chain structures of two types of PDAA polymer bases.

Polymer	PDAA formed with CrO$_3$ as oxidant	PDAA formed with K$_2$CrO$_4$ as oxidant
C/H/N/O/S/total [wt%]	65.1/3.47/10.72/13.45[a]/0/92.74	61.8/3.09/10.59/13.45[a]/0.5[b]/89.43
experimental formula	C$_{14}$H$_{6.64}$N$_{1.98}$O$_2$	C$_{14}$H$_{4.98}$N$_{2.09}$O$_2$
calculated formula	C$_{14}$H$_{6.67}$N$_2$O$_2$	C$_{14}$H$_5$N$_2$O$_2$
proposed chain structure		

[a] The calculated value from the monomer. [b] An impurity from the remnant dopant.
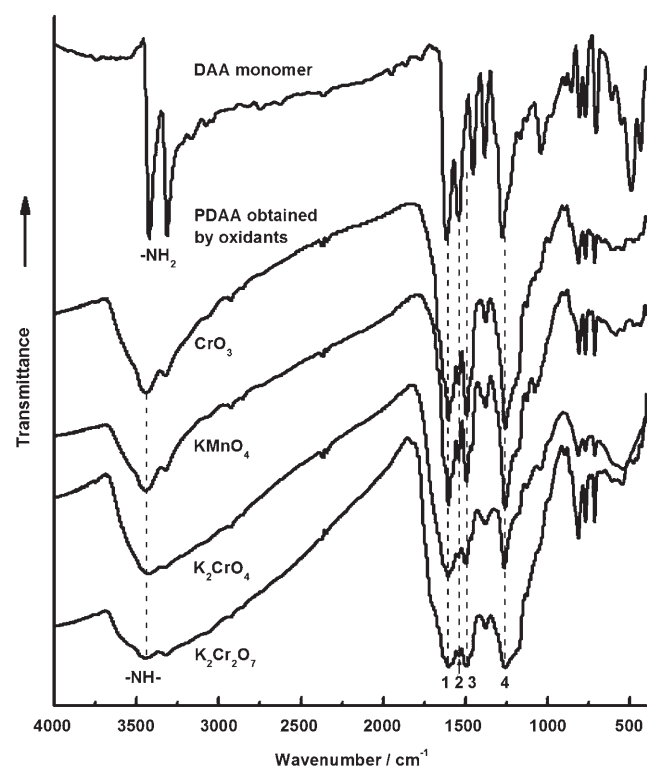

Figure 4. IR spectra of the DAA monomer and PDAA polymer salts prepared with an oxidant/DAA monomer molar ratio of 1:1 in 1 M H$_2$SO$_4$ in DMF at 20 °C for 24 h. Band assignments: 1: C=O, 2: C=C quinoid, 3: C=C benzenoid, 4: C–N.

Their similar partial ladder chain structures have also been proved by similar WAXD characteristics in Figure 6.

The FTIR spectra of the DAA monomer and PDAA polymer obtained by the chemically oxidative polymerization are illustrated in Figure 4. A strong doublet due to NH$_2$ stretching at approximately 3420 and 3314 cm^{-1} in the spectrum of the monomer has turned into a broad singlet centered at around 3440 cm^{-1} in the spectra of the four PDAAs. A moderate absorption at 496 cm^{-1} due to C–C–NH$_2$ bend in the DAA monomer has become much weaker in the spectra of the four PDAAs. These changes strongly suggest

that a large amount of free NH$_2$ groups have changed into NH groups after the polymerization. Other strong bands at 1614 cm^{-1} assigned to C=O stretching, 1547 cm^{-1} assigned to the anthraquinone ring, and 1277 cm^{-1} assigned to C–N stretching all shift to lower wavenumbers for the four PDAAs. In particular, the broader band due to C=C stretching in the quinoid ring of the PDAAs could overlap with the band for C=O stretching at 1614 cm^{-1}. With such a structural feature of PDAA, two types of redox reactions can simultaneously occur in the polymer: reversible redox reactions for the π-conjugated polymer and for the quinone groups.[19] Large differences between the IR spectra of the monomer and the polymer, as well as the quinoid and benzenoid structures of the polymerization products, indicate that the polymerization products are not a simple complex or mixture of monomers with some oligomers. In fact, this is evidence for the formation of a real polymer.

The UV/Vis absorption spectra of the DAA monomer and polymers in NMP (see Figure S3 in the Supporting Information and Table 3) suggest that all four PDAAs exhibit quite different UV/Vis spectra to that of the monomer. A strong band at 262–278 nm due to the π→π* transition in quinonediimine-like units is observed for both the DAA monomer and PDAAs. The strongest band centered at 488 nm, due to quinone groups, has become a moderate band at 486–500 nm for the four PDAAs.[20] The PDAAs obtained with K$_2$Cr$_2$O$_7$ and K$_2$CrO$_4$ demonstrate very weak UV/Vis absorbance at 608 and 622 nm, respectively, because of their low solubility in NMP and also their weakly π-con-

Table 3. The UV/Vis maximum band wavelengths and their intensity ratios for PDAA polymers synthesized with the four oxidants at five polymerization temperatures.

	Maximal wavelength [nm]			Intensity ratio of band c/a
	band a	band b	band c	
oxidants at 20 °C:				
DAA monomer (no oxidant)	270	488	–	0
CrO$_3$	263	496	632	0.34
KMnO$_4$	266	500	625	0.35
K$_2$CrO$_4$	262	512	622	0.10
K$_2$Cr$_2$O$_7$	262	528	608	0.12
polymerization T [°C] with CrO$_3$ as oxidant:				
0	263	492	627	0.28
10	262	496	631	0.30
20	263	496	632	0.34
35	263	500	626	0.25
50	262	500	617	0.22

jugated structure. The PDAAs obtained with CrO_3 and $KMnO_4$ display a unique band at 632 or 625 nm, respectively, which corresponds to the n→π* transition of the π-conjugated system in polyaniline-like units,[6] because this band disappeared in the UV/Vis spectrum of the DAA monomer. So great a difference between the UV/Vis spectra of the DAA monomer and PDAA polymers must be attributed to a strong polymerization effect. In other words, the black solid powders obtained by the chemical oxidative polymerization are indeed polymers.

It can easily be found from a comparison of the UV/Vis spectra in Figure S3 in the Supporting Information with the band data in Table 3 that the band c wavelength increases steadily and regularly upon changing of oxidant from $K_2Cr_2O_7$ to K_2CrO_4, $KMnO_4$, and CrO_3. This increasing order basically coincides with the conductivity increase in Table 1. The much higher intensity ratio of band c/band a of PDAAs obtained with $KMnO_4$ and CrO_3 verifies their much higher conductivity relative to that of those obtained with $K_2Cr_2O_7$ and K_2CrO_4. Therefore, it is certain that CrO_3 is the best oxidant of the four effective oxidants for the synthesis of PDAA with the highest yield/conductivity and also the longest conjugation length.

With CrO_3 fixed as the oxidant, it is found from Figure S3 (right) in the Supporting Information that the UV/Vis spectra of the PDAAs vary significantly with the polymerization temperature. With elevation of the temperature from 0–50 °C, both the band c wavelength and band c/band a intensity ratio exhibit maxima at 20 °C, as listed in Table 3, a result implying that the PDAA obtained at 20 °C possesses the longest conjugated length. This further confirms that the highest conductivity is achieved at 20 °C (Figure 3).

A high-resolution solid-state ^{13}C NMR spectrum of the PDAA oxidized by CrO_3 is shown in Figure 5. The ^{13}C NMR spectrum is characterized by two types of signals, which correspond to carbonyl aromatic carbon atoms (sharp) and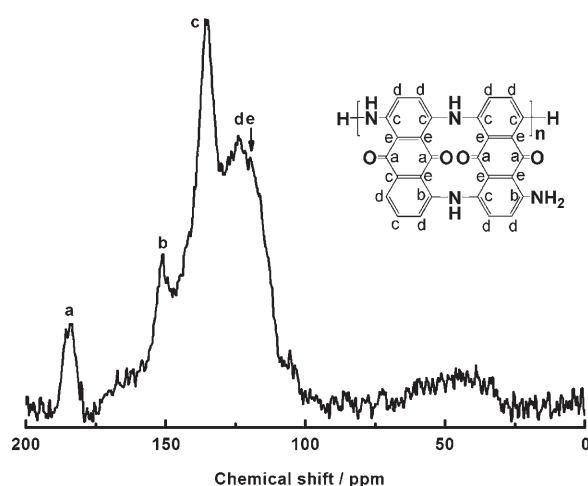 normal aromatic carbon atoms (broad). The broad peaks in a wide range between $\delta = 100$–175 ppm must be attributed to the skeleton of all the aromatic carbon atoms except for the carbonyl aromatic carbon atoms. Although it is difficult to make an exact assignment for the aromatic carbon atoms, a possible peak assignment has been given in Figure 5 based on the calculated chemical shifts for a model hexamer oligomer by CS Chem Ultra 8.0 (see Figure S4 in the Supporting Information) and also the elemental analysis results in Table 2. A partial ladder chain of the PDAA is proved again.

WAXD diffraction analysis reveals that the PDAA particles obtained with CrO_3, $K_2Cr_2O_7$, K_2CrO_4, and $KMnO_4$ are substantially amorphous, as shown in Figure 6. The traces
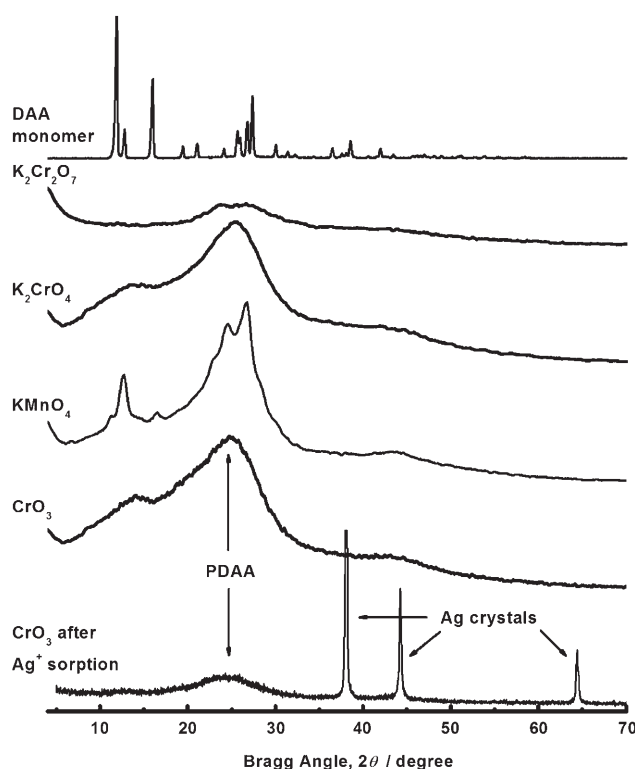

Figure 6. WAXD diffractograms of DAA monomer and PDAA salt particles prepared with an oxidant/DAA monomer molar ratio of 1:1 in 1 M H_2SO_4 in DMF at 20 °C for 24 h.

consist mainly of an intense broad peak, a shoulder peak, and a weak peak at Bragg angles of around 20°, 13°, and 44°, respectively. These broad diffractograms are typical characteristics of an amorphous polymer. PDAA oxidized by $K_2Cr_2O_7$ appears to be the most amorphous, whereas PDAA oxidized by $KMnO_4$ is the most crystalline, although the absolute crystallinity of the latter is still low. Furthermore, PDAA obtained with $K_2Cr_2O_7$ exhibits a stronger diffraction peak at approximately 3° than the peak at 25°, a result indicating the presence of larger ordered sizes. Therefore, it can be concluded that the four PDAA salts possess amorphous structures on the whole, which are quite different from the highly crystalline structures of the DAA mono-

Figure 5. Solid-state high-resolution ^{13}C NMR spectrum and possible assignment for PDAA polymer salt prepared with a CrO_3/DAA monomer molar ratio of 1:1 in 1 M H_2SO_4 in DMF at 20 °C for 24 h.

mer (top trace in Figure 6), DAA oligomers, and DAA complexes.[21,22a] This is also important evidence for the formation of a real oxidative polymer.

Particle size analysis: Figure 7 shows the size and its distribution for PDAA particles (in water) synthesized in H_2SO_4/DMF without any external emulsifier or stabilizer at five
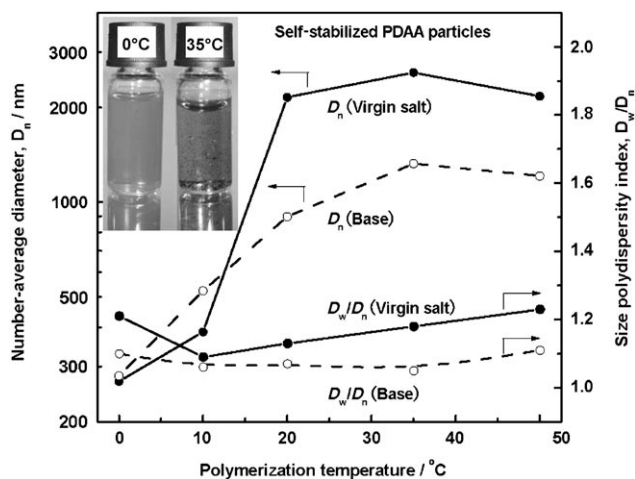

Figure 7. Variation of the number-average diameter (D_n) and size polydispersity index (D_w/D_n) of PDAA virgin salt and base particles (in water) fabricated at five polymerization temperatures with a CrO_3/DAA molar ratio of 1:1 in 1 M H_2SO_4/DMF for 24 h, as detected by laser particle-size analysis. The inset shows the dispersions of the nanoparticles (left) and microparticles (right) of the PDAA virgin salts prepared at 0 °C and 35 °C in water.

polymerization temperatures. A significant influence of polymerization temperature on the size of the PDAA particles has been observed. The number-average diameter (D_n) exhibits a decreasing tendency for virgin salt and base of the PDAA particles upon lowering of polymerization temperature from 40 to 0 °C. In particular, the salt and base particles formed at 0 °C are the smallest, with D_n values of 269 and 280 nm, respectively. The size polydispersity index (D_w/D_n) of the PDAA salt and base particles is very small, ranging from 1.05–1.23, an indication of a narrow size distribution of the particles. Indeed, the dispersion in pure water of the PDAA particles formed at 35 °C looks like a suspension, as shown in the inset of Figure 7, while the dispersion of the PDAA particles formed at 0 °C looks like a homogeneous solution. This basically implies that the former is microparticles[22b] and the latter is nanoparticles because the PDAA particles are completely insoluble in water. The D_n and D_w/D_n values of the PDAA base particles formed at 20–50 °C are ordinarily smaller than those of the corresponding salt particles, because a dedoping treatment in NH_4OH would eliminate the external dopant and then result in a tight arrangement of the polymer chains and, furthermore, in size uniformization of the resulting base particles. The D_n values of the PDAA base particles formed at 0–10 °C are slightly larger than those of corresponding salt particles, because

very small dedoped base particles with much less charge would exhibit relatively low stability, thereby leading to a conglomeration to some extent. Possibly, the effect of polymerization temperature on the particle size may primarily be ascribed to interference at the doping level of the PDAA particles.

The morphology of the PDAA salt particles fabricated at 0 °C has been observed with transmission electron microscopy (TEM) and field-emission scanning electron microscopy (FE-SEM) in Figure 8. The PDAA salt particles look like
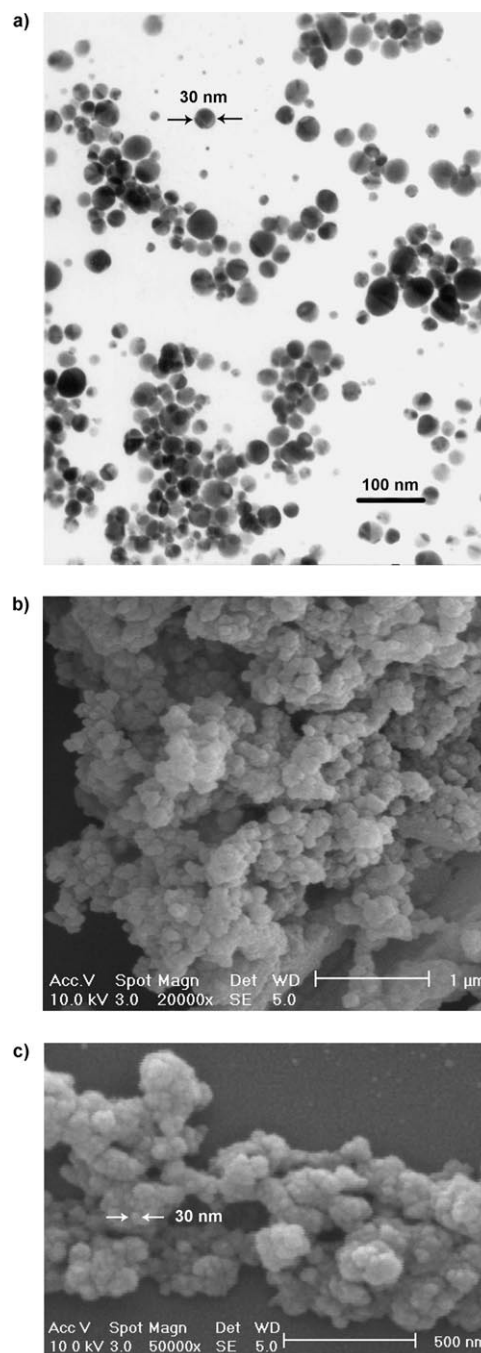

Figure 8. a) TEM and b,c) FE-SEM images of PDAA polymer salt particles prepared with a CrO_3/DAA molar ratio of 1:1 in 1 M H_2SO_4 in DMF at 0 °C for 24 h.

nanospheres with an average diameter of around 30 nm, with the largest and smallest diameters being 45 and 12 nm, respectively. A similar particle size of around 30 nm has also been proved by FE-SEM observations. It should be noticed that the particle size revealed by FE-SEM and TEM is much smaller than that determined by laser particle-size analysis (LPA), which may be due to contraction and compression of the particles after the exclusion of DMF and water inside the particles during the drying for electron microscopic observations. That is to say, the TEM and FE-SEM samples are in the equilibrium dry state under vacuum, whereas the LPA samples are filled with water or even DMF.

Generally, polyaniline particles formed by conventional oxidative polymerization in the absence of external stabilizers are microparticles with an average size of around 4–16 µm.[23,24] It is reported that polyaniline nanofibers tend to be formed by using interfacial or rapidly mixed syntheses without any stabilizer.[25] However, polyaniline spherical nanoparticles could not be facilely obtained without external stabilizer. It seems that the external stabilizer is crucial to the productive synthesis of nanometer or even submicrometer polyaniline spherical particles by polymerization; this leads to impure nanoparticles with a complicated composition due to the contamination with a large amount of the external stabilizer. However, if sulfonic groups or quinoline nitrogen atoms are incorporated into the polymer chains as internal stabilizers, submicrometer or even nanometer particles of conducting polymers from aniline and its derivatives can be fabricated in situ by oxidative precipitation polymerization without any external stabilizer.[15,18] In this study, PDAA nanoparticles have apparently been successfully prepared by a simple polymerization of DAA monomer excluding any sulfonic groups or quinoline nitrogen atoms in acidic DMF without any external stabilizer. A possible reason for the formation and self-stabilization of the PDAA nanoparticles could be the lone electron pair on the oxygen atom of the quinone group, which might generate C–O$^-$ to make the polymer chain display a negative charge, as shown in Scheme 1.[6] Static repulsion between the negative charges
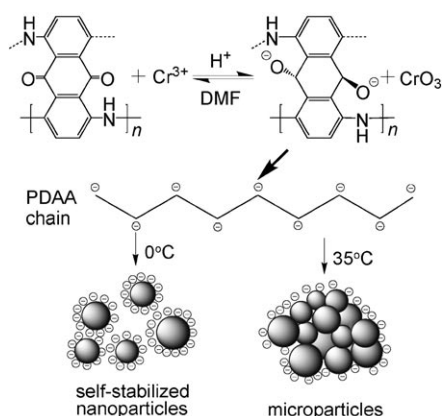
Scheme 1. Possible stabilization mechanism of PDAA polymer salt particles (in H$_2$SO$_4$/DMF or water at pH 5.5) obtained with CrO$_3$/DAA monomer in a molar ratio of 1:1 in 1 M H$_2$SO$_4$/DMF for 24 h.

might stabilize the as-formed nanoparticles by preventing them from conglomeration. Furthermore, this stabilization mechanism has been confirmed by a charged-adduct effect on the negatively charged PDAA nanoparticle surface. It can be seen from Figure 9 that a dispersion of the PDAA nanoparticles in an electrolyte solution of 1 M aqueous NaCl will precipitate completely after 24 h, while a dispersion of the PDAA nanoparticles in water medium at pH 5.5 remains consistently stable. A similar destabilization has been observed for a polyaniline nanofiber dispersion in acidic NaCl aqueous solution.[26] This phenomenon could be explained by the classical Derjaguin–Landau–Verwey–Overbeek (DLVO) theory.[27] Therefore, the PDAA nanoparticles are able to exist stably in a polymerization medium such as acidic DMF or even water at pH 5.5. The nanoparticles obtained here should have high purity and clean surfaces because 1) no external stabilizer or dispersant was added into the polymerization system and 2) DMF, dissociative H$_2$SO$_4$, residual DAA, CrO$_3$, and its acidic reducing product Cr$_2$(SO$_4$)$_3$ in/on the nanoparticles have been totally removed by centrifugation with water.
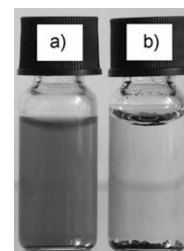

Figure 9. Dispersion of PDAA salt nanoparticles in a) water at pH 5.5 and b) 1 M NaCl after standing for 24 h at 25 °C.

Properties of the PDAA polymers

Solubility: It can be seen from Table 1 that the solubility of the PDAA particles in some representative solvents with various dielectric constants depends significantly on the oxidants used for the polymerization. Generally, concentrated H$_2$SO$_4$, HCOOH, DMSO, NMP, and *m*-cresol with high dielectric constants are good solvents for the polymers. The solubility consistently becomes better in formic acid, DMSO, NMP, *m*-cresol, THF, and CHCl$_3$ if the oxidant is changed from K$_2$Cr$_2$O$_7$ and K$_2$CrO$_4$ to CrO$_3$ to KMnO$_4$, possibly due to more NH/NH$_2$ groups or a reduced chain structure of the PDAAs obtained with CrO$_3$ and KMnO$_4$. The PDAAs oxidized by K$_2$Cr$_2$O$_7$ and K$_2$CrO$_4$ always exhibit the lowest solubility in the chosen solvents because they have fewer NH/NH$_2$ groups or an oxidized chain structure (Table 2). The four PDAAs exhibit a gradually decreased solubility in solvents with decreasing dielectric constants, except for the water, HCl, and NaOH aqueous solutions. The solubility of the PDAA polymers can also vary with the polymerization conditions. The PDAA polymers obtained with CrO$_3$ are more soluble under lower oxidant/monomer ratio, higher polymerization temperature, and higher acid concentration (see Table S2 in the Supporting Information). However, the PDAAs obtained in the five acids/DMF seem to exhibit the same solubility, that is, they are soluble in H$_2$SO$_4$, partly soluble in HCOOH, DMSO, NMP, and *m*-cresol, but only slightly soluble in THF and chloroform (see Table S1 in the

Supporting Information). An exception is that the PDAA obtained in H_3PO_4 is mainly soluble in HCOOH. Obviously, very low solubility or complete insolubility of the PDAA polymers in THF, $CHCl_3$, or the HCl and NaOH aqueous solutions will signify good chemical resistance to apolar organic solvents or strong acid/base aqueous media, which could be very beneficial for silver-ion adsorption in waste water containing apolar organic solvents and strong acids/bases.

Solvatochromism: It is interesting that a color variation of the PDAA polymer solution is observed with the different solvents, that is, there is a novel solvatochromism. As listed in Table 1 and in Tables S1 and S2 in the Supporting Information, the polymer solution exhibits different colors in various solvents. Almost all of the PDAA polymers are often black in H_2SO_4, green in HCOOH, and blue or bluish purple in NMP, DMSO, and *m*-cresol. That is to say, the PDAA might exist as different chain conformations or even configurations in various solvents. However, the PDAA solution colors hardly ever change with variation in the polymerization conditions, including oxidant species, oxidant/DAA ratio, polymerization temperature, acid species, and acid concentration.

Bulk electrical conductivity: The PDAA particles are an electrical semiconductor like other aromatic diamine polymers obtained by oxidative polymerization. As listed in Table 1, the bulk electrical conductivity of the PDAAs in three states significantly changes with the oxidant species. The PDAAs formed with CrO_3 as the oxidant exhibit the highest conductivity, and the polymer formed with $KMnO_4$ shows the second highest conductivity. If $K_2Cr_2O_7$ is used as the oxidant, the conductivity of the PDAA polymers seems to be the lowest. This phenomenon coincides with the UV/Vis spectral results (see Figure S3 in the Supporting Information). As illustrated in Figures 1–3, the conductivity of all of the PDAAs increases first and then decreases upon changing the oxidant/monomer ratio, polymerization temperature, and H_2SO_4 concentration. The conductivity of virgin PDAA salts increases gradually from 1.12×10^{-9} to 9.65×10^{-8}, 5.78×10^{-7}, 5.54×10^{-6}, and 9.87×10^{-6} $S\,cm^{-1}$ with the variation from H_3PO_4 to HNO_3, HCl, H_2SO_4, and $HClO_4$ as the polymerization acid media in DMF. Of all PDAAs in the three redox states, $HClO_4$-redoped salts always demonstrate the highest conductivity, up to 5.45×10^{-5} $S\,cm^{-1}$, whereas NH_4OH dedoped bases always demonstrate the lowest conductivity. In other words, $HClO_4$-redoped PDAA salts always exhibit much higher conductivity than virgin PDAA salts in H_2SO_4, HCl, HNO_3, and H_3PO_4, possibly due to the higher doping ability of $HClO_4$. In addition, it can be seen from Figures 2 and 7 that the smallest nanoparticles of the PDAA virgin salts fabricated at 0 °C have the lowest conductivity because of their largest interface resistance and most localized electrons.[28] Therefore, it can be concluded that the PDAAs exhibit the maximal conductivity when CrO_3 acts as the oxidant and $HClO_4$ is used

as the redopant with a 1:1 oxidant/monomer molar ratio at 20 °C in 1 M H_2SO_4/DMF. This indicates that the conductivity is very sensitive to the polymerization and doping conditions because the redox state, molecular weight, and π-conjugation length of the PDAAs are dramatically influenced by the polymerization conditions. In other words, the conductivity could be efficiently optimized by controlling and regulating the polymerization and doping conditions. The remarkable variation in the conductivity and solubility of the PDAAs with different oxidant species suggests quite different chain structures.

Thermal stability: The PDAA polymers obtained previously by electropolymerization are well known as electrode materials for supercapacitors or rechargeable batteries. Here we report three types of new important properties of the polymers formed by chemically oxidative polymerization, including thermal, photoluminescent, and silver-ion sorptive properties. The differential scanning calorimetry (DSC) curve of the PDAA base particles is shown in Figure 10a. It seems that no endothermic transition was observed, whereas two sharp exothermic peaks centered at 449 and 466 °C clearly appeared. In other words, the PDAA particles did not exhibit any thermal transition, such as glass or melting transitions, before their thermal degradation. The first major exothermic peak is most likely attributed to the breakage of the main chain, while the second minor exothermic peak is mostly due to the combustion of residual char formed after
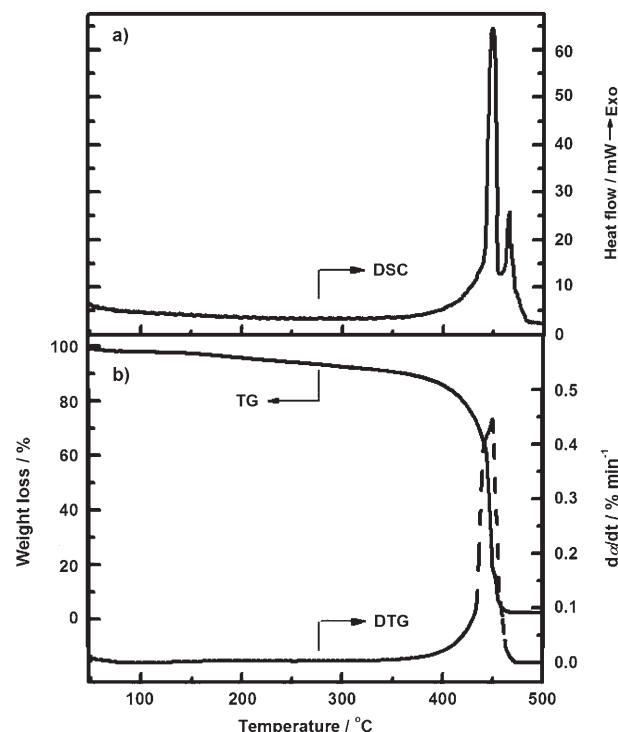

Figure 10. DSC, TG, and DTG curves in an air atmosphere for the PDAA salt particles prepared with a CrO_3/DAA molar ratio of 1:1 in 1 M H_2SO_4/DMF at 20 °C for 24 h.

the PDAA decomposition. Thermal gravimetric (TG) and differential thermal gravimetric (DTG) analyses were conducted to analyze the thermal stability of the PDAA base particles. As shown in Figure 10b, only one major weight loss was observed at around 450 °C, a result indicating main-chain decomposition of the polymer. In an air atmosphere, the PDAA was completely decomposed at 460 °C. There was no residual powder left in the sample pan after the TG test. The decomposition temperature determined by the TG/DTG method is substantially consistent with the exothermic temperatures observed by DSC. The thermal analyses indicated that the PDAA base powders exhibit a high thermal stability at temperatures below 400 °C because of the high aromaticity and rigidity of the PDAA skeletons.

Photoluminescence: The photoluminescence characteristics, including the excitation and emission spectra of the DAA monomer and PDAA polymer nanoparticles in several media, are shown in Figure 11. Apparently, the excitation and emission spectra are quite different from each other. All excitation spectra exhibited a strong band in a range of 239–309 nm, which corresponds to the $\pi \rightarrow \pi^*$ electronic transition. The double bands in NMP and ethanol are characteristic of many π-conjugated polymers and arise from a distribution of conjugation lengths. The emission spectra, which are assigned to the radiative decay of singlet excitons, have a more pronounced vibronic structure and exhibit a

maximum in the range of 344–418 nm. The shape, position, and intensity of the excitation and emission spectra of the PDAA nanoparticles differ significantly from those of the DAA monomer.[29] In particular, the excitation and emission intensities of the PDAA nanoparticles in NMP, due to fluorescence reinforcement by polyaniline-like π-conjugated chains, are almost six times stronger than those of DAA monomer at the same concentration in NMP. This phenomenon reflects the fact that the molecular structure of PDAA nanoparticles is quite different from that of the DAA monomer. This can also be treated as more evidence for the formation of a true PDAA polymer.

Some excitation and emission peaks in Figure 11 were blue or red shifted, depending on the medium employed. Excitation and emission are greatly influenced by solvent polarity because it perturbs the fundamental and excited state of the polymer. An excited state with a highly polar character will interact with media of high polarity to stabilize the excited state on a low energy level, hence causing a red shift of the emission. A blue shift is expected for solvents of low polarity. The PDAA polymer in this study shows a strong optical dependence upon the medium around it. The photoluminescence emission maximum of the PDAA nanoparticles shifts to longer wavelengths from 344 to 375 to 418 nm as the dielectric constant of the medium increases from 25 (ethanol) to 32 (NMP) to 80 (water). A similar effect has also been revealed for other polymers; these results indicate that the excited state of the PDAA polymer has a polar structure that is highly influenced by the dipole of the medium.[30,31]
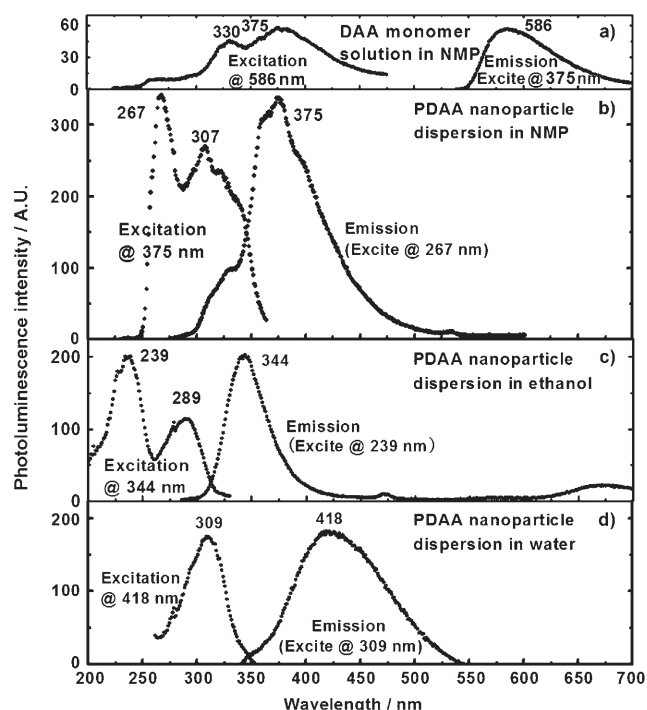

Figure 11. Excitation and emission scans for a) the DAA monomer solution in NMP and b–d) PDAA salt nanoparticles dispersed in NMP (b), ethanol (c), and water (d) at the same concentration of 12.5 mg L^{-1}. The PDAA nanoparticles are partly soluble in NMP.

Silver-ion sorption: As summarized in Table 4, the Ag$^+$ adsorbability onto the PDAA particles is strongly affected by the oxidant species and polymerization temperature or particle size. First of all, the DAA monomer containing two NH$_2$ groups without any -NH-/-N= groups does not possess any Ag$^+$ adsorbability. This implies that the oxidizability of the Ag$^+$ ion is not strong enough to effectively oxidize the DAA monomer for a reductive sorption of the Ag$^+$ ion onto it. The PDAA particles obtained by K$_2$Cr$_2$O$_7$ have medium Ag$^+$ adsorbability due to the presence of -NH-/-N= groups on the PDAA with a certain molecular weight that is confirmed by the π-conjugated structure (see Table 3 and the Supporting Information) and semiconductivity (Table 1). The PDAA particles formed by K$_2$CrO$_4$ and KMnO$_4$ exhibit stronger Ag$^+$ adsorbability, which is proved by higher conductivity of Ag$^+$-adsorbing particles. The PDAA particles synthesized by CrO$_3$ demonstrate the strongest Ag$^+$ adsorbability besides their high polymerization yield and good insolubility in common organic solvents and acid/base aqueous media. The different adsorbability of PDAAs oxidized by different oxidants may be ascribed to the different contents of -NH$_2$/-NH-/-N= groups or the different redox or doping (salt)/dedoping (base) states, possibly due to different interactions between the Ag$^+$ ions and polymer chains with different chain structures.[32] In particular, all of the PDAA base particles possess higher adsorbability than the corre-

Table 4. Silver-ion adsorption onto virgin salts and bases of PDAA particles synthesized by chemical oxidative polymerization with different oxidants in 1 M H_2SO_4/DMF for 24 h. The adsorption of Ag^+ ions was performed in 83.1 mM $AgNO_3$ solution (25 mL) at 30°C with particle sorbent (50 mg) for an adsorption time of 24 h in the absence of ultrasonic treatment.

Oxidant	Polymerization T [°C]	Ag^+ adsorbance [mg g^{-1}]		Ag^+ adsorptivity [%]		Conductivity after Ag^+ sorption [S cm^{-1}]	
		salt	base	salt	base	salt	base
$K_2Cr_2O_7$	20	184.5	219.6	4.13	4.9	6.37×10^{-6}	1.45×10^{-7}
K_2CrO_4	20	220.4	320.7	4.9	7.14	1.24×10^{-5}	8.91×10^{-6}
$KMnO_4$	20	212.0	249.5	4.69	5.53	2.38×10^{-5}	1.02×10^{-5}
CrO_3	20	242.7	322.5	6.24	7.35	5.28×10^{-5}	3.58×10^{-5}
CrO_3	20	283.2[a]		7.3[a]		6.21×10^{-5}[a]	
CrO_3	0	365.0	376.2	9.4	9.6	3.54×10^{-5}	1.63×10^{-5}
CrO_3	0	485.4[a]	582.5[a]	12.5[a]	15.0[a]	7.35×10^{-5}[a]	2.13×10^{-5}[a]

[a] PDAA salt nanoparticles were ultrasonically treated during the initial 1 h of Ag^+ sorption.

tive sorption of Ag^+ on the particles may be regarded as an efficient doping method for the preparation of conducting materials.

Conclusions

Fine PDAA particles have been successfully synthesized by a facile chemical oxidative polymerization. The polymerization yield, macromolecular and morphological structures, bulk electrical conductivity, and solubility of the particles are fundamentally influenced by the oxidant species, oxidant/monomer molar ratio, polymerization temperature, acid species, and concentration. This indicates that the polymerization characteristics, structure, and properties of the polymers could be controlled or even optimized by regulating the polymerization conditions. The upmost conductivity would be achieved when CrO_3 acts as the oxidant at a CrO_3/DAA molar ratio of 1:1 in 1 M H_2SO_4/DMF medium at 20°C. The systematic characterization of the structure and properties suggests that the oxidative products obtained are genuine polymers that are remarkably different from the previously reported DAA complex with metal ions. Partial ladder chain structures with reduced and oxidized states were proposed for the PDAA polymers with CrO_3 and K_2CrO_4 as oxidants, respectively, based on a careful comparison of the elemental analysis and ^{13}C NMR spectrum. The particle size of the PDAA polymers could be considerably controlled by optimizing the polymerization temperature and doping/dedoping treatment. The size of the PDAA salt particles decreases steadily with lowering polymerization temperature. Novel PDAA nanoparticles with a mean diameter of around 30 nm, high purity, intrinsic conductivity, and strong self-stability have been successfully fabricated by chemical oxidative polymerization with a CrO_3/DAA molar ratio of 1:1 in 1 M H_2SO_4/DMF medium at 0°C, which is a very facile method of synthesizing pure nanoparticles because no external stabilizer or interior sulfonic group is needed. The negatively charged quinone groups might be vital for the formation and stable existence of the nanoparticles. The PDAA nanoparticles exhibit two unique nanoeffects, namely strong fluorescence and strong silver-ion adsorbability, together with good chemical and heat resistance. These effects endow the particles with wide potential applications as photoluminescent materials and as advanced sorbents in the removal and recycling of noble or heavy metallic ions from waste water. Furthermore, it can be predicted that PDAA polymers adsorbing silver particles could serve as novel modifiers for electrode materials, due to their reinforced electrochemical activity, strong charge–discharge capacity,[6,34] and extensively adjustable conductivity over a range of seven

sponding salts, and the maximal adsorbance and adsorptivity could reach up to 582.5 mg g^{-1} and 15%, respectively, enhancements of 20 and 20% compared with the PDAA salt particles. The enhanced adsorbability may be attributed to exclusion of doping sulfuric acid and the formation of more bare amino/imino (-NH$_2$/-NH-/-N=) groups on the polymer chains. Furthermore, PDAA nanoparticles synthesized at 0°C by CrO_3 demonstrate much stronger Ag^+ adsorbability and their Ag^+ adsorbance and adsorptivity values are 1.5 times higher than those of microparticles synthesized at 20°C. Furthermore, the ultrasonically treated particles exhibit even stronger Ag^+ adsorbability because of their better dispersion. The strong Ag^+ adsorbability onto the PDAA nanoparticles should be attributed to their outstanding nanoeffects. That is to say, the smaller PDAA particles usually exhibit higher Ag^+ adsorbability because of having a much larger specific area.[33] Therefore, it could be inferred that the adsorption of the Ag^+ onto the PDAA particles can follow two adsorption mechanisms: 1) a complex mechanism between Ag^+ ions and the -NH$_2$/-NH-/-N= groups of the polymer and 2) a redox mechanism between Ag^+ ions (as the oxidant) and -NH$_2$/-NH- groups (as the reductant).

It is seen from Tables 1 and 4 that the conductivity of the virgin salt and base of PDAA particles formed at 20°C increases around 10-fold, as compared with the Ag-free particles, after Ag^+ sorption for 24 h (Figure 2). It is interesting that the conductivity of the Ag-adsorbing particles is nearly the same as that of $HClO_4$-redoped particles (Table 1). In particular, the virgin salt PDAA nanoparticles formed at 0°C exhibit around 1000-times higher conductivity after Ag^+ adsorption than the Ag-free particles (Figure 2). The enhanced conductivity can be explained by the growing and doping mechanism of reduced Ag crystals, the presence of which has been confirmed by their three much stronger typical diffraction peaks at 38°, 44°, and 64° (Figure 6), respectively, corresponding to the (111), (200), and (220) lattice planes of the Ag crystals. Remarkably increased conductivity of the virgin salt PDAA nanoparticles after Ag^+ sorption must be attributed to their much higher Ag^+ adsorbance than that of PDAA microparticles. Consequently, the reac-

orders of magnitude, as expected. Finally, the PDAA polymers have demonstrated unique versatility.

Experimental Section

Reagents: 1,5-Diaminoanthraquinone (DAA), CrO_3, $K_2Cr_2O_7$, K_2CrO_4, $KMnO_4$, H_2SO_4, HCl, $HClO_4$, HNO_3, H_3PO_4, $AgNO_3$, formic acid, DMF, *m*-cresol, dimethylsulfoxide (DMSO), *N*-methylpyrrolidone (NMP), chloroform, THF were commercially obtained as chemical pure reagents and used without further purification.

Chemical oxidative polymerization of the DAA monomer: The DAA polymers were prepared by chemical oxidative polymerization of the DAA monomers. A typical procedure for the preparation of DAA polymer is as follows: DAA (1.19 g, 5 mmol) was added to H_2SO_4 nonaqueous medium in DMF (1.0 M, 60 mL) in a 250 mL glass flask in a water bath at 20 °C and the mixture was then stirred vigorously for half an hour. An oxidant solution was prepared separately by dissolving CrO_3 (1.16 g, 5 mmol) in H_2SO_4 in DMF (1.0 M, 10 mL). The DAA monomer solution was then treated with the CrO_3 oxidant solution by dropwise addition of the CrO_3 solution at a rate of 1 drop (around 60 μL) per 3 s. The reaction mixture was stirred continuously for 24 h at 20 °C, with measurement of the open circuit potential (OCP) and temperature of the polymerization solution. After that, the polymer salt particles as precipitates were isolated from the reaction mixture by filtration and washed with ethanol and an excess of distilled water in order to remove the remaining monomer, oxidant, and oligomers. A part of the polymer salt was subsequently neutralized in ammonium hydroxide (0.2 M, 100 mL) with stirring overnight. All of the final polymer particles were left to dry in ambient air for 1 week. The DAA polymers were obtained as black solid powders that are quite different from the dark red DAA monomer (see Figure S1 in the Supporting Information). The black color is a characteristic indication of the polymer having a largely π-conjugated chain structure, a fact that has been further verified by the following results of UV/Vis spectroscopy and moderate electrical conductivity.

Measurements: The DAA polymerization was followed by the OCP profile technique, by using a saturated calomel electrode (SCE) as the reference electrode and a Pt electrode as the working electrode. The elemental analysis of PDAA bases was carried out on a Carlo Erba 1106 element analyzer. IR spectra were recorded on KBr pellets on a Nicolet Magna-IR 550 spectrometer at 2 cm^{-1} resolution. The high-resolution solid-state ^{13}C NMR spectrum was recorded by using Varian Infinity Plus 300 spectrometer operating at 75.5 MHz. The UV/Vis spectra of DAA polymers at a concentration of 12.5 mgL^{-1} in NMP were recorded on a Lambda 35 UV/Vis spectrophotometer (Perkin–Elmer Instruments) at a wavelength range of 700–200 nm at a scanning rate of 480 nm min^{-1}. Fluorescence intensity measurements were carried out on a Cary Eclipse fluorescence spectrophotometer (Varian Australia Pty Ltd, Victoria, Australia) with a spectral slit width at 5 nm. Wide-angle X-ray diffraction (WAXD) was performed with a Bruker D8 Advance X-ray diffractometer made in Germany with $Cu_{K\alpha}$ radiation at a scanning rate of 0.888° min^{-1}. The size and its distribution of the as-formed (salt) and NH_4OH-treated (base) particles of the PDAA polymers were analyzed on a Beckman Coulter LS230 laser particle-size analyzer. The size and morphology of the particles were further observed by a Hitachi model H600 transmission electron microscope and a field-emission scanning electron microscope (Philips XL30 FEG). The polymer solubility was evaluated as follows: polymer powder (2 mg) was added to solvent (1 mL) and dispersed thoroughly by shaking intermittently for 2 h at ambient temperature. The bulk electrical conductivities of the salt and base of the DAA polymers were measured by the following method: polymer powders (10 mg) were placed between two round-disk stainless iron electrodes with a diameter of 1 cm and the powder was pressed tightly to form a pellet. The resistance and thickness of the polymer pellet were then measured with a multimeter and a thickness gauge, respectively. DSC and TG measurements were performed in static air with a sample size of 3 mg at a temperature range from room temperature to 800 °C

and at a heating rate of 10 °C min^{-1} by using a Pyris 1 DSC & TGA Perkin–Elmer thermal analyzer. The sorption of Ag$^+$ ions in aqueous solution onto the DAA polymer particles was performed in a batch experiment. Ag$^+$ solution (25 mL) at an Ag$^+$ concentration of 83.1 mM was incubated with a given amount of the particles at a fixed temperature of 30 °C. After a desired treatment period, the particles were filtered from the solution and then the concentration of Ag$^+$ in the filtrate was measured by Volhard titration. The adsorbed amount of Ag$^+$ ions on the microparticles was calculated according to Equations (1) and (2), in which Q is the adsorption capacity, q is the adsorptivity, C_0 and C are the Ag$^+$ concentrations before and after adsorption, respectively, V is the initial volume of the Ag$^+$ solution, M is the molecular weight of the Ag$^+$ ions, and W is the weight of the microparticles added.

$$Q = (C_0 - C)VM/W \tag{1}$$

$$q = [(C_0 - C)/C_0] \times 100 \tag{2}$$

Acknowledgement

[1] a) S. Shreepathi, R. Holze, *Chem. Mater.* **2005**, *17*, 4078; b) G. Trippé, F. L. Derf, J. Lyskawa, M. Mazari, J. Roncali, A. Gorgues, E. Levillain, M. Sallé, *Chem. Eur. J.* **2004**, *10*, 6497.

[2] X. G. Li, M. R. Huang, W. Duan, Y. L. Yang, *Chem. Rev.* **2002**, *102*, 2925.

[3] A. G. MacDiarmid, *Angew. Chem.* **2001**, *113*, 2649; *Angew. Chem. Int. Ed.* **2001**, *40*, 2581.

[4] X. Y. Zhang, S. K. Manohar, *J. Am. Chem. Soc.* **2005**, *127*, 14156.

[5] a) C. Jérôme, S. Demoustier-Champagne, R. Legras, R. Jérôme, *Chem. Eur. J.* **2000**, *6*, 3089; b) R. J. Tseng, J. X. Huang, J. Y. Ouyang, R. B. Kaner, Y. Yang, *Nano Lett.* **2005**, *5*, 1077.

[6] K. Naoi, S. Suematsu, A. Manago, *J. Electrochem. Soc.* **2000**, *147*, 420.

[7] a) K. Naoi, S. Suematsu, M. Hanada, H. Takenouchi, *J. Electrochem. Soc.* **2002**, *149*, 472; b) V. K. Gater, M. D. Love, M. D. Liu, C. R. Leidner, *J. Electroanal. Chem. Interfacial Electrochem.* **1987**, *235*, 381.

[8] S. A. Hashmi, S. Suematsu, K. Naoi, *J. Power Sources* **2004**, *137*, 145.

[9] P. Banerjee, B. M. Mandal, *Macromolecules* **1995**, *28*, 3940.

[10] B. Wessling, J. Posdorfer, *Synth. Met.* **1999**, *102*, 1400.

[11] B. Wessling, *Synth. Met.* **2003**, *135–136*, 265.

[12] a) X. G. Li, R. Liu, M. R. Huang, *Chem. Mater.* **2005**, *17*, 5411; b) X. G. Li, M. R. Huang, S. X. Li, *Acta Mater.* **2004**, *52*, 5363; c) M. R. Huang, Q. Y. Peng, X. G. Li, *Chem. Eur. J.* **2006**, *12*, 4341.

[13] X. Y. Zhang, A. G. MacDiarmid, S. K. Manohar, *Chem. Commun.* **2005**, 5328.

[14] Y. Wei, K. F. Hsueh, G. W. Jang, *Polymer* **1994**, *35*, 3572.

[15] X. G. Li, M. R. Huang, Y. M. Hua, *Macromolecules* **2005**, *38*, 4211.

[16] E. Erdem, M. Karakisla, M. Sacak, *Eur. Polym. J.* **2004**, *40*, 785.

[17] Y. Cao, A. Andreatta, A. J. Heeger, P. Smith, *Polymer* **1989**, *30*, 2305.

[18] a) X. G. Li, H. J. Zhou, M. R. Huang, M. F. Zhu, Y. M. Chen, *J. Polym. Sci. Part A* **2004**, *42*, 3380; b) X. G. Li, Q. F. Lü, M. R. Huang, *Chem. Eur. J.* **2006**, *12*, 1349.

[19] S. Suematsu, K. Naoi, *J. Power Sources* **2001**, *97*, 816.

[20] T. Yamamoto, H. Etori, *Macromolecules* **1995**, *28*, 3371.

[21] K. Alagesan, A. G. Samuelson, *Synth. Met.* **1997**, *87*, 37.

[22] a) M. N. Vijayashree, S. V. Subramanyam, A. G. Samuelson, *Macromolecules* **1992**, *25*, 2988; b) G. X. Xu, L. Qi, L. Wen, G. Q. Liu, Y. X. Ci, *Acta Polym. Sin.* **2006**, 795.

[23] G. Min, *Synth. Met.* **2001**, *119*, 273.

[24] J. X. Huang, R. B. Kaner, *Angew. Chem.* **2004**, *116*, 5941; *Angew. Chem. Int. Ed.* **2004**, *43*, 5817.

[25] J. X. Huang, R. B. Kaner, *Chem. Commun.* **2006**, 367.

[26] D. Li, R. B. Kaner, *Chem. Commun.* **2005**, 3286.

[27] R. J. Hunter, *Foundations of Colloid Science, Vol. 1*, Oxford University Press, New York, **1987**.

[28] H. S. Xia, Q. Wang, *J. Nanopart. Res.* **2001**, *3*, 401.

[29] M. Umadevi, V. Ramakrishnan, *J. Raman Spectrosc.* **2003**, *34*, 13.

[30] L. O. Palsson, C. Wang, D. L. Russel, A. P. Monkman, M. R. Bryce, G. Rumbles, I. D. W. Samuel, *Chem. Phys.* **2002**, *279*, 229.

[31] F. Huang, H. Wu, D. Wang, W. Yang, Y. Cao, *Chem. Mater.* **2004**, *16*, 708.

[32] J. A. Smith, M. Josowicz, J. Janata, *J. Electrochem. Soc.* **2003**, *150*, E384.

[33] X. N. An, H. M. Zeng, *Carbon* **2003**, *41*, 2889.

[34] J. E. Park, S. G. Park, A. Koukitu, O. Hatozaki, N. Oyama, *J. Electrochem. Soc.* **2003**, *150*, 959.